Journal of Virology

# Cytomegalovirus Destruction of Focal Adhesions Revealed in a High-Throughput Western Blot Analysis of Cellular Protein Expression

**R. J. Stanton, B. P. McSharry, C. R. Rickards, E. C. Y. Wang, P. Tomasec and G. W. G. Wilkinson**

***J. Virol.*** **2007, 81(15):7860. DOI: 10.1128/JVI.02247-06.**
**Published Ahead of Print 23 May 2007.**

JOURNAL OF VIROLOGY, Aug. 2007, p. 7860–7872 Vol. 81, No. 15
0022-538X/07/$08.00+0 doi:10.1128/JVI.02247-06


# Cytomegalovirus Destruction of Focal Adhesions Revealed in a High-Throughput Western Blot Analysis of Cellular Protein Expression†▽

R. J. Stanton,[1]* B. P. McSharry,[1] C. R. Rickards,[1] E. C. Y. Wang,[2] P. Tomasec,[1] and G. W. G. Wilkinson[1]

*Department of Medical Microbiology[1] and Department of Medical Biochemistry and Immunology,[2] Wales School of Medicine, Cardiff University, Cardiff, United Kingdom*

Received 13 October 2006/Accepted 14 May 2007

**Human cytomegalovirus (HCMV) systematically manages the expression of cellular functions, rather than exerting the global shutoff of host cell protein synthesis commonly observed with other herpesviruses during the lytic cycle. While microarray technology has provided remarkable insights into viral control of the cellular transcriptome, HCMV is known to encode multiple mechanisms for posttranscriptional and posttranslation regulation of cellular gene expression. High-throughput Western blotting (BD Biosciences Powerblot technology) with 1,009 characterized antibodies was therefore used to analyze and compare the effects of infection with attenuated high-passage strain AD169 and virulent low-passage strain Toledo at 72 hpi across gels run in triplicate for each sample. Six hundred ninety-four proteins gave a positive signal in the screen, of which 68 from strain AD169 and 71 from strain Toledo were defined as being either positively or negatively regulated by infection with the highest level of confidence (BD parameters). In follow-up analyses, a subset of proteins was selected on the basis of the magnitude of the observed effect or their potential to contribute to defense against immune recognition. In analyses performed at 24, 72, and 144 hpi, connexin 43 was efficiently downregulated during HCMV infection, implying a breakdown of intercellular communication. Mitosis-associated protein Eg-5 was found to be differentially upregulated in the AD169 and Toledo strains of HCMV. Focal adhesions link the actin cytoskeleton to the extracellular matrix and have key roles in initiating signaling pathways and substrate adhesion and regulating cell migration. HCMV suppressed expression of the focal-adhesion-associated proteins Hic-5, paxillin, and α-actinin. Focal adhesions were clearly disrupted in HCMV-infected fibroblasts, with their associated intracellular and extracellular proteins being dispersed. Powerblot shows potential for rapid screening of the cellular proteome during HCMV infection.**

Human cytomegalovirus (HCMV) is a clinically important herpesvirus associated with severe disease following congenital infection and in immunocompromised individuals. As a herpesvirus, primary infection is accompanied by lifelong persistence during which the infection must be controlled by continuous host immune surveillance. HCMV has the largest genome of any characterized human virus (~236 kb) and is predicted to encode on the order of 165 potential open reading frames (15). Systematic deletion of individual open reading frames from the Towne strain revealed that only 45 are essential for virus replication in vitro; thus, accessory genes account for most of the HCMV coding capacity (16). While the functions of most of these genes have not been determined, a significant number have been implicated in the targeting of both the innate and adaptive host immune responses (40). HCMV has also recently been shown to express microRNAs during productive infection that also have the potential to modulate host cell gene expression (17, 21, 43). A high-throughput proteomic approach was used in this study with a view to providing further insight into how the virus may modulate its host cell.

HCMV replicates slowly in permissive human fibroblasts, with gene expression conventionally being divided into three phases: immediate-early (IE), early, and late (reviewed in reference 40). Early-phase transcription precedes viral DNA replication (initiates at 16 to 24 h postinfection [hpi]), with significant virus production detected from 72 hpi and peaking at approximately 144 hpi. Productive HCMV infection is associated with an overall stimulation of both cellular transcription and translation (50). Virion binding (13, 59), release of virion tegument proteins following virion fusion (6, 36), and de novo expression of powerful transcriptional regulators (most notably, IE2 and IE1) during infection all modulate cellular gene expression. Following infection, while cellular proteins associated with DNA metabolism are induced, host cell cyclins are dysregulated and licensing of host cell DNA replication is inhibited, resulting in a "pseudo-$G_1$" environment compatible with efficient virus DNA replication (3, 5, 25). Microarray experiments have proved highly informative in revealing the dynamic regulation of steady-state levels of cellular transcripts, both positively and negatively, during the course of infection (7, 26, 48, 65, 66). HCMV is known not only to regulate transcriptional initiation but also to control RNA processing (1, 9, 14, 20, 35, 63), translation, and posttranslational modification and protein trafficking (31, 34, 44, 54, 61). The result of many of these processes is liable to be an alteration of host cell protein levels.

* Corresponding author. Mailing address: Department of Medical Microbiology, Tenovus Building, Heath Park, Cardiff CF14 4XX, United Kingdom. Phone: 44 29 20744521. Fax: 44 29 20746449. E-mail: stantonrj@cf.ac.uk.

† Supplemental material for this article may be found at http://jvi.asm.org/.

▽ Published ahead of print on 23 May 2007.

TABLE 1. Parameters used by BD to assign confidence levels to changes in protein expression

| Level | Description |
|---|---|
| 10 | Changes of greater than 2-fold in 9 of 9 comparisons from good-quality signals that pass visual inspection[c] |
| 9 | Changes of 1.5- to 1.9-fold in 9 of 9 comparisons from good-quality signals that pass visual inspection[c] |
| 8 | Changes of greater than 2-fold in 9 of 9 comparisons from low-quality signals[a] that pass visual inspection[c] |
| 7 | Changes of 1.25- to 1.5-fold in 9 of 9 comparisons from good-quality signals |
| 6 | Changes of greater than 2-fold in 9 of 9 comparisons from good-quality signals that do not pass visual inspection[c] |
| 5 | Changes of 1.5- to 1.9-fold in 9 of 9 comparisons from good-quality signals that do not pass visual inspection[c] |
| 4 | Changes of greater than 2-fold in 9 of 9 comparisons from low-quality signals[a] that do not pass visual inspection[c] |
| 3 | Low-signal data,[b] changes of 1.5- to 1.9-fold in 9 of 9 comparisons |
| 2 | Low-signal data,[b] changes of 1.25- to 1.49-fold in 9 of 9 comparisons |
| 1a | Changes of greater than 2-fold in 8 of 9 comparisons |
| 1b | Changes of 1.5- to 1.9-fold in 8 of 9 comparisons |

[a] Low- versus high-quality signals are determined by analysis software and are not subject to technician judgment.
[b] Low-signal data are for signals with a normalized quantity of <500 or low quality. Results can be inconsistent.
[c] Visual inspection is done by a technician, and there are instances when a band (signal) is not visible to the human eye but is still discerned by the analysis software. A greater confidence value is assigned when a visual inspection can confirm the software-based determination, so when the technician is unable to see the band a lower confidence level is assigned to the signal.

While HCMV strains AD169 and Towne are used extensively in research, their genomes are recognized to have accumulated genetic defects during extensive passage in vitro, the most substantial being a deletion of a 13- to 15-kb sequence designated UL/*b′* (11, 15). Vaccine trials have indicated that the genetic alterations accrued by the laboratory strains have rendered them relatively avirulent, whereas a limited-passage Toledo strain showed virulence characteristics in early passages (45). The characterized strain Toledo UL/*b′* sequence has at some stage undergone a sequence inversion that inactivates UL128, a gene required for endothelial tropism. Repairing the deletion in the Towne strain with the strain Toledo UL/*b′* sequence was not sufficient to restore virulence (24), yet it did confer a much enhanced capacity to resist natural killer cell (NK) recognition (54). The UL/*b′* sequence has been predicted to encode 23 additional open reading frames, including genes implicated in regulating viral tropism (UL128 to UL131A) (15, 23) and immune modulation, including two chemokine homologues (UL146, UL147) (42, 49) and a tumor necrosis factor receptor homologue (UL144) (2), and confers remarkable protection against NK attack (10, 58) associated with the NK evasion functions UL141 and UL142 (12, 54, 57, 62). In HCMV-infected cells, posttranslational control of cellular ligands is a major factor in both promoting and evading NK recognition. HCMV encodes at least four genes that act posttranslationally to suppress cell surface major histocompatibility complex class I expression, UL40 donates a peptide that enables maturation of HLA-E, and gpUL16 binds to and prevents maturation of NKG2D ligands, while gpUL141 binds to nectin-like molecule 5 (Necl-5/CD155/PVR), preventing its maturation (34, 53, 54, 61). In order to gain further insight into the effect of HCMV infection on host defenses, we used Powerblot (BD Biosciences) technology to evaluate the overall effects of HCMV infection on the cellular proteome.

The Powerblot system uses an inventory of 1,009 monoclonal antibodies to evaluate the relative levels of protein expression in a high-throughput immunoblotting assay. To allow time for changes to be manifested, lysates were prepared from strain AD169-infected, strain Toledo-infected, and mock-infected fibroblasts at 72 hpi. Triplicate samples were analyzed on separate polyacrylamide gels. Following immunoblotting, positive signals were measured with an infrared capture system and densitometry measurements were performed. Pairwise comparisons adjusted by compensation with normalized controls provided a quantitative readout that was further checked by visual inspection. Powerblot technology was used to identify cellular proteins whose expression is modulated positively and negatively during productive infection. In follow-up studies to validate the technology, we observed a clear effect on proteins implicated in the regulation of intercellular interactions. In this context, HCMV was observed to suppress the expression of multiple cellular proteins involved in focal adhesion (α-actinin, paxillin, Hic-5) and connexin junctions (connexin 43).

## MATERIALS AND METHODS

**BD Powerblot.** Human fetal foreskin fibroblasts (HFFF) were mock infected or infected with HCMV strain Toledo or AD169 at a multiplicity of infection (MOI) of 5. At 72 hpi, whole cells were lysed in boiling lysis buffer (10 mM Tris, pH 7.4, 1 mM sodium orthovanadate, 1% sodium dodecyl sulfate [SDS]) containing protease inhibitor cocktail (P8340; Sigma), sonicated, frozen at −80°C, and sent to BD Biosciences on dry ice for analysis.

BD separated all of the samples on a 0.5-mm-thick 4 to 15% gradient SDS-polyacrylamide gel. Samples equivalent to approximately 8 μg per lane were loaded, and the gel was run for 1.5 h at 150 V. Samples were transferred with a wet-transfer TE series (Hoefer) to Immobilon-P membrane (Millipore) for 2 h at 200 mA. For antibody detection, the membrane was blocked for 1 h with blocking buffer (LI-COR) and clamped with a Western blotting manifold that isolated 40 channels across the membrane. In each channel, a complex antibody cocktail was added and allowed to hybridize for 1 h at 37°C. The blot was removed from the manifold, washed, and hybridized for 30 min at 37°C with secondary goat anti-mouse antibody conjugated to Alexa Fluor 680 fluorescent dye (Molecular Probes) and goat anti-rabbit antibody conjugated to IRDye 800 fluorescent dye (Rockland). The membrane was washed, dried, and scanned at 700 nm (for monoclonal antibody target detection) and 800 nm (for polyclonal antibody target detection) with the Odyssey infrared imaging system (LI-COR). Molecular weight standards were loaded with two standardization cocktails.

BD performed densitometry analysis of the detected bands. These readings were normalized to the sum intensity of all of the valid spots on a blot and then multiplied by 1,000,000, and the molecular weight was determined. Analysis was provided in the form of pairwise comparisons for each protein between each pair of samples. This was performed between triplicate readings for each sample, giving a three-by-three comparison matrix for each pair of proteins. These comparisons were then ranked on the basis of the size of the change observed, the reproducibility of that change between the triplicate repeats, and the absolute strength or quality of the signal on the polyvinylidene difluoride membrane. These analyses were performed both by computer analysis and by visual inspection of the membranes. In this manner, changes were ranked into 10 levels (Table 1). For the Powerblot data obtained in this study, see Fig. SA to SD in the supplemental material.

**Cells and virus.** HFFF were infected with HCMV for 2 h with rocking, following which the cells were washed with phosphate-buffered saline (PBS) and fresh medium was added. Virus strain Toledo (kindly provided by E. S. Mocarski), AD169, or an AD169 mutant which expresses green fluorescent protein (GFP) under the control of the β-2.7 early promoter (AD169-GFP) (39) was used. Virus stocks were prepared from HFFF infected with the required virus. Tissue culture supernatants were kept when a 100% cytopathic effect (CPE) was observed and were centrifuged to remove cell debris. Cell-free virus was pelleted from supernatant by centrifugation at 22,000 × *g* for 2 h and then resuspended in fresh Dulbecco modified Eagle medium.

**Western blotting.** HFFF were mock infected or infected (MOI of 5) with HCMV strain Towne or AD169, and samples were harvested exactly as for the Powerblot but additional time points were taken (24, 72, and 144 hpi). Protein concentration estimation was performed with the bicinchoninic acid protein assay reagent (Pierce) according to the manufacturer's instructions, and an 8-μg sample was run per lane. Samples were diluted in 2× SDS loading buffer (250 mM Tris, pH 6.8, 2% [wt/vol] SDS, 10% [vol/vol] glycerol, 100 mM dithiothreitol, 0.1% [wt/vol] bromophenol blue), and SDS-polyacrylamide gel electrophoresis was performed (46).

Gels were blotted onto polyvinylidene difluoride membrane (Amersham), and prestained molecular weight standards (Rainbow Marker; Amersham) were used to monitor protein transfer. Membranes were blocked for 1 h in blocking buffer (5% dried milk, 0.1% Tween 20 in PBS) before being incubated for an hour in primary antibody diluted in blocking buffer. Membranes were washed for 30 min with three changes of washing buffer (0.1% Tween 20 in PBS), and incubated with horseradish peroxidase-conjugated secondary antibody (1:1,000 dilution; Amersham) for an hour. Another 30-min wash, with three changes of wash buffer, was performed, and samples were reacted with SuperSignal reagent (Pierce). Primary anti-Hic-5 (61164), anti-Eg5 (61186), anti-RIG-G (611244), anti-paxillin (P49620), anti-α-actinin (612576), anti-FAK (610087), and anti-connexin 43 (610061) monoclonal antibodies were obtained from BD Biosciences and used at the recommended dilutions. Anti-CD29 (21270291S) and anti-CD49e (21336491S) antibodies were obtained from Immunotools and used at a 1:10 dilution.

Luminescence was detected with the Autochemi system (UVP), and densitometry measurements were made with Labworks 4.5 software (UVP). All measurements were taken from original images without any destructive image processing, and all measurements for any single antibody were taken simultaneously. Measurements from any single antibody are therefore comparable.

**Immunofluorescence.** With the exception of focal-adhesion-associated proteins, all immunofluorescence analysis was performed at 48 hpi to minimize binding to the Fc receptors expressed strongly by HCMV at later time points in infection. Cells were fixed for 15 min in 2% paraformaldehyde, washed in PBS, and then permeabilized in 0.5% NP-40 for 15 min. Cells were incubated with primary antibody for 1 h at 37°C, washed, and incubated for 1 h at 37°C with secondary antibody before being washed and mounted in 2% 1,4-diazabicyclo[2.2.2]octane (DABCO). Primary antibodies were the same as for Western blotting (see above) and were again used at the manufacturer-recommended dilution. The secondary antibody was goat anti-mouse Alexa Fluor 594 conjugate (Molecular Probes) used at 1:5,000.

For imaging of focal-adhesion proteins, cells were grown on fibronectin-covered coverslips. Ten micrograms of fibronectin (Sigma) was added to the coverslips, and they were incubated overnight at 4°C. The coverslips were washed, and the cells were allowed to adhere. Cells were grown in 2% fetal calf serum to prevent overgrowth, infected as described above, and stained at 72 hpi. To prevent reactions with Fc receptors, the secondary antibody was chicken anti-mouse Alexa Fluor 594 conjugate (Molecular Probes) used at 1:1,000.

4′,6′-Diamidino-2-phenylindole (DAPI; Sigma) was added to the secondary antibody at a final concentration of 1 μg/ml. Images were viewed on a Leica DM-IRBE microscope at a magnification of ×630 with a Hamamatsu ORCA-ER camera and processed with Openlab 3 (Improvision).

## RESULTS

**Powerblot.** In total, 1,009 antibodies were used in the Powerblot to analyze expression from HFFF that were mock infected or infected with strain AD169 or Toledo. HCMV infection is recognized to stimulate cellular metabolism while simultaneously dysregulating normal cell cycle progression. In contrast, control cells will continue to progress through the cell cycle, divide, and eventually become growth inhibited when reaching confluence. This situation needs always to be borne in mind when comparing HCMV-infected cells with uninfected controls. The mass of both uninfected and infected cells will change over time. As infected cells are unable to divide, there are fewer cells each with a higher protein content, relative to mock-infected controls. Total-protein measurements of cell extracts analyzed in the Powerblot showed that levels in infected cells were 1.6 to 1.9 times those of mock-infected controls (Table 2). Since the amount of protein applied in each sample was constant, a protein whose expression remains unchanged in absolute abundance in an infected cell will thus decrease in relative abundance compared to that in an uninfected cell. However, such a decrease in "relative abundance" may also have an impact on function. In this study, this issue was circumvented by focusing on proteins that underwent a greater-than-twofold change in abundance (i.e., confidence levels 1a, 4, 8, and 10 as defined by BD parameters; Table 1) as a consequence of infection. Lysed samples were run on SDS-polyacrylamide gel electrophoresis in triplicate and Western blotted before being probed with multiple antibody cocktails, each containing five to eight antibodies which recognize proteins of differing molecular masses. Following binding with a secondary antibody, data were captured with an infrared capture system and densitometry measurements were performed on the triplicate samples. Pairwise comparisons were performed between every pair of samples, with changes expressed as + or − and as an *n*-fold change compared to normalized controls. Of the 1,009 antibodies, 837 were designated as reacting with human proteins and of these, 686 to 694 proteins of the expected molecular mass were recognized in any one cellular extract. A visual comparison is included within BD's scoring system (Table 1). Despite built-in compensation, disparity in transfer or antibody-binding efficiency within some blots was manifested as a variation between scores in the set of nine pairwise comparisons for each individual protein (see Fig. SA to SD in the supplemental material).

TABLE 2. Protein concentrations of whole-cell lysates sent to BD for Powerblot analysis

| Samples | Protein concn (mg/ml) |
|---|---|
| Mock-infected HFFF | 0.299 |
| Strain AD169-infected HFFF | 0.466 |
| Strain Toledo-infected HFFF | 0.567 |

A total of 71 (Toledo-infected versus mock-infected cells), 68 (strain AD169-infected versus mock-infected cells), or 13 (strain Toledo-infected versus strain AD169-infected cells) proteins changed with the highest confidence level (level 10) (see Fig. SB to SD in the supplemental material). A comparison identified a set of 37 proteins that changed with level 10 confidence in both the strain Toledo-versus-mock-infected cell and strain AD169-versus-mock-infected cell comparisons. A significant number of proteins clearly exhibited a confidence level 10 change with only one of the viruses. When evaluated individually, these proteins that were observed to change (+ or −) substantially with one virus often also changed similarly with the other strain, but with a confidence change lower than level 10. In nearly all of the cases, this was due to variation between the triplicate repeats in one of the comparisons pre-

TABLE 3. Proteins selected for follow-up analysis

| Protein | Comment | HCMV-induced change according to Powerblot |
|---|---|---|
| Connexin 43 | Enables intercellular communication | Downregulation |
| Eg5 | Regulates mitotic-spindle formation | Upregulation |
| FXR2 | Fragile X mental retardation autosomal homolog | Upregulation[a] |
| Hic-5 | Focal-adhesion-associated protein | Downregulation |
| hILP/XIAP | Inhibitor of apoptosis | Upregulation |
| hPRP17 | Splicing factor | Upregulation[a] |
| Paxillin | Focal-adhesion-associated protein | Downregulation |
| RIG-G | Retinoic-acid-induced gene G | Upregulation |
| ZAG | Zn-α2-glycoprotein, related to class I major histocompatibility complex | Downregulation[a] |

[a] Not confirmed in follow-up.

venting an accurate and reliable *n*-fold change reading being derived. Thus, while we focused in this study on proteins modulated with level 10 confidence, further examination of the Powerblot data can be expected to identify more cellular proteins differentially modulated by HCMV infection. Nevertheless, upon examining the level 10 proteins for all three comparisons, we found a bias for protein increases in the infected cells compared to controls; 39 (57%) of 68 (strain AD169-infected versus mock-infected cells) and 45 (63%) of 71 (Toledo-infected versus mock-infected cells) level 10 proteins showed increases rather than decreases in the comparisons.

**Validation of Powerblot data.** A subset of nine proteins shown to be modulated by HCMV infection in the Powerblot experiment was selected for further analysis by conventional Western blotting (Table 3). In the follow-up study, duplicate mock-infected control samples were used and cell extracts were collected at 24, 72, and 144 hpi. Care was taken to ensure that the same amount of protein was loaded for each sample. Total protein concentrations were determined in a standard chemical assay (see Materials and Methods) and checked by performing densitometric measurements on Coomassie blue-stained SDS-polyacrylamide gel electrophoresis gels (data not shown). For all of the proteins examined, the monoclonal antibody was the same designation as that used in the Powerblot.

All nine of the proteins selected for follow-up exhibited level 10 significance changes between virus-infected and mock-infected cells and provided strong signals in the Powerblot. However, no difference in expression level was observed between virus- and mock-infected cells for three of the nine proteins (FXR2, hPRP17, and ZAG) in a follow-up Western analysis (Table 3). Proteins FXR2 and hPRP17 were not detected at substantial levels in any sample in the follow-up Western analysis (data not shown), while for the Zn-α2 glycoprotein (ZAG), the signal was attributed to a breakdown product of a higher-molecular-weight protein detected by a different antibody in the Powerblot cocktail. For the remaining six proteins, good concordance was seen between follow-up analysis and the Powerblot. Four of these proteins were analyzed further because their modulation indicated that HCMV infection may be having a specific effect on focal adhesions and intercellular communication; this selection thus allowed us to test the predictive power of the Powerblot.

**Connexin 43.** Gap junctions form pores between cells which are in direct contact and enable cell-to-cell communication via the transmission of ions and other small molecules. Connexin 43 is one of a family of connexins (the only one found in fibroblasts) which form these gap junctions when they self-oligomerize into hexameric structures, surrounding a central aqueous pore. Intracellular transport through a gap junction potentially could be detrimental to HCMV if, for example, it facilitated the transfer of interferons. The Powerblot indicated that connexin 43 was efficiently downregulated by infection with both HCMV strains (Fig. 1A). Follow-up analysis supported the Powerblot result. Indeed, connexin 43 downregulation was apparent by 24 hpi, with levels dropping below detectability at 144 hpi (Fig. 1A and B). Comparable levels of downregulation were observed with strains AD169 and Toledo.

Fibroblasts did not readily form gap junctions in in vitro culture, even in confluent monolayers. Immunofluorescence analysis shows that connexin 43 was predominantly associated with characteristic intracellular structures in uninfected cells that are thought to be associated with storage (H. Evans, personal communication). Figure 1C shows that by 48 hpi, not only was the overall level of connexin 43 reduced but the associated cytoplasmic structures became less prominent, to the point that in some infected cells they were not detectable.

**Eg5.** Eg5 is a kinesin-related protein that regulates spindle formation at the centrosome, ensuring appropriate distribution of duplicated chromosomes between daughter cells (4). Eg5 was not detected by Powerblot in mock-infected cells, yet it was expressed at high levels following HCMV infection. In the conventional Western blot assay, Eg5 was detected at 24 h in mock-infected cells but declined over time as cells became confluent, in line with its recognized role in mitosis (18) (Fig. 2A and B). At 24 hpi, Eg5 was expressed at comparable levels in the HCMV-infected and mock-infected cell extracts. While Eg5 declined in control cells, it was sustained (strain Toledo) or enhanced (strain AD169) as the infection progressed (Fig. 2A and B). This is best observed directly when the 24- and 144-h time points are compared directly (Fig. 2C).

In contrast to mock-infected cells, infection with HCMV strain AD169 induced strong upregulation of Eg5 at both 72 and 144 hpi. The situation is more complex with strain Toledo, where in contrast to the Powerblot, the upregulation of Eg5 was less than that observed with strain AD169 and represents a difference that was consistent across experimental repeats (data not shown) in the modulation of cellular gene expression by these two HCMV strains that was not apparent in the Powerblot.

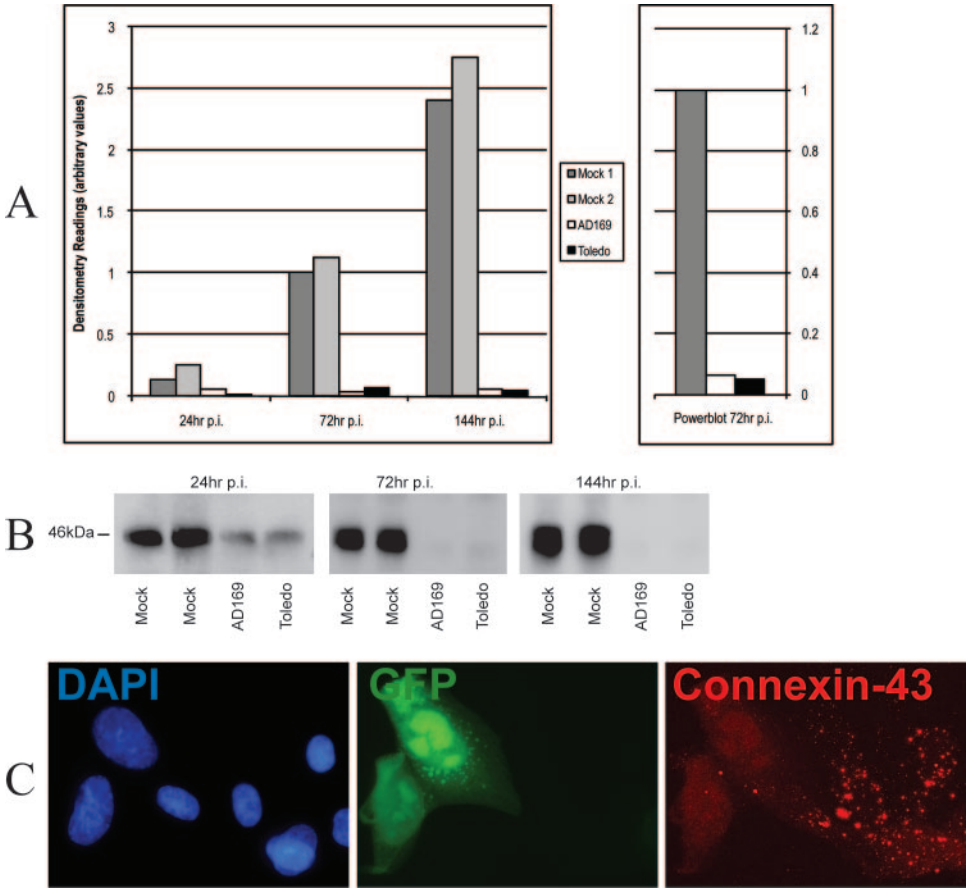


FIG. 1. Analysis of connexin 43 expression. (A) Densitometry measurements from conventional Western blot assays (MOI = 5) are shown on the left side of the graph, and those from the Powerblot (MOI = 5) are on the right. (B) Conventional Western blot assays from which measurements were taken (MOI = 5). (C) Immunofluorescence assay performed on HFFF infected 48 h previously (MOI = 0.5) with strain AD169-GFP such that infected cells appear green. Cells were stained with DAPI to locate the nuclei of all of the cells (blue) and for connexin 43 (red).

HCMV infection is associated with the accumulation of the mitotic cyclin-dependent kinase (cdk) cdk1/cyclin B1 complex. Furthermore, HCMV infection has been associated with the induction of a "pseudomitotic" state that involves the formation of spindle poles and abnormal chromosome condensation in a proportion of the cells. The sustained expression of Eg-5 may be related to aberrant activation of cell cyclins, whereas cell division in control cells becomes constrained by confluence inhibition, suppressing Eg-5 levels.

Eg5 levels are increased, even in nondividing neurons, at points where changes in cellular architecture are occurring (18). Immunofluorescence studies were therefore carried out to examine Eg-5 localization in infected cells (Fig. 2D). A low MOI was used to enable comparison with uninfected cells in the same field. Enhanced levels of Eg5 staining were detected in strain AD169-infected cells; however, there was no obvious localization with specific intracellular structures. An identical staining pattern was seen at a high MOI and at both low and high MOIs with strain Toledo-infected cells (data not shown).

**Paxillin.** Focal adhesions are membrane nucleation sites where actin filaments are linked to the extracellular matrix via an integrin bridge. Paxillin is a cytoskeletal protein associated with focal adhesions that is subjected to extensive tyrosine phosphorylation as a consequence of changes in cell adhesion and morphology (56). Powerblot detected two major forms of paxillin that differentially migrate with apparent molecular masses of 58 and 68 kDa. Of these, only the 58-kDa form changed significantly, showing a sevenfold (strain AD169) or fivefold (strain Toledo) reduction in expression levels at 72 h compared to mock-infected cells (see Fig. SB and SC in the supplemental material; Fig. 3A). The major 58-kDa form and the minor 68-kDa species were also apparent in the follow-up conventional Western blot analysis, as well as a 46-kDa form. Infection with strains AD169 and Toledo caused fourfold and sevenfold reductions, respectively, at 72 hpi compared to the mock-infected control if only the predominant 58-kDa species is considered, while the 46-kDa species was not detectable in infected cells after 24 h. Mock-infected cells showed a decrease in paxillin levels at 144 hpi such that strain AD169-infected levels were comparable to those of mock-infected cells at this time point. Paxillin levels were lower in strain Toledo-infected cells than in strain AD169-infected cells; thus, levels were still reduced, relative to those in mock-infected cells, at 144 h in strain Toledo-infected cells.

Immunofluorescence analysis revealed a clear difference between cells infected with a strain AD169 virus and mock-infected controls (Fig. 3C). Focal adhesions are more clearly

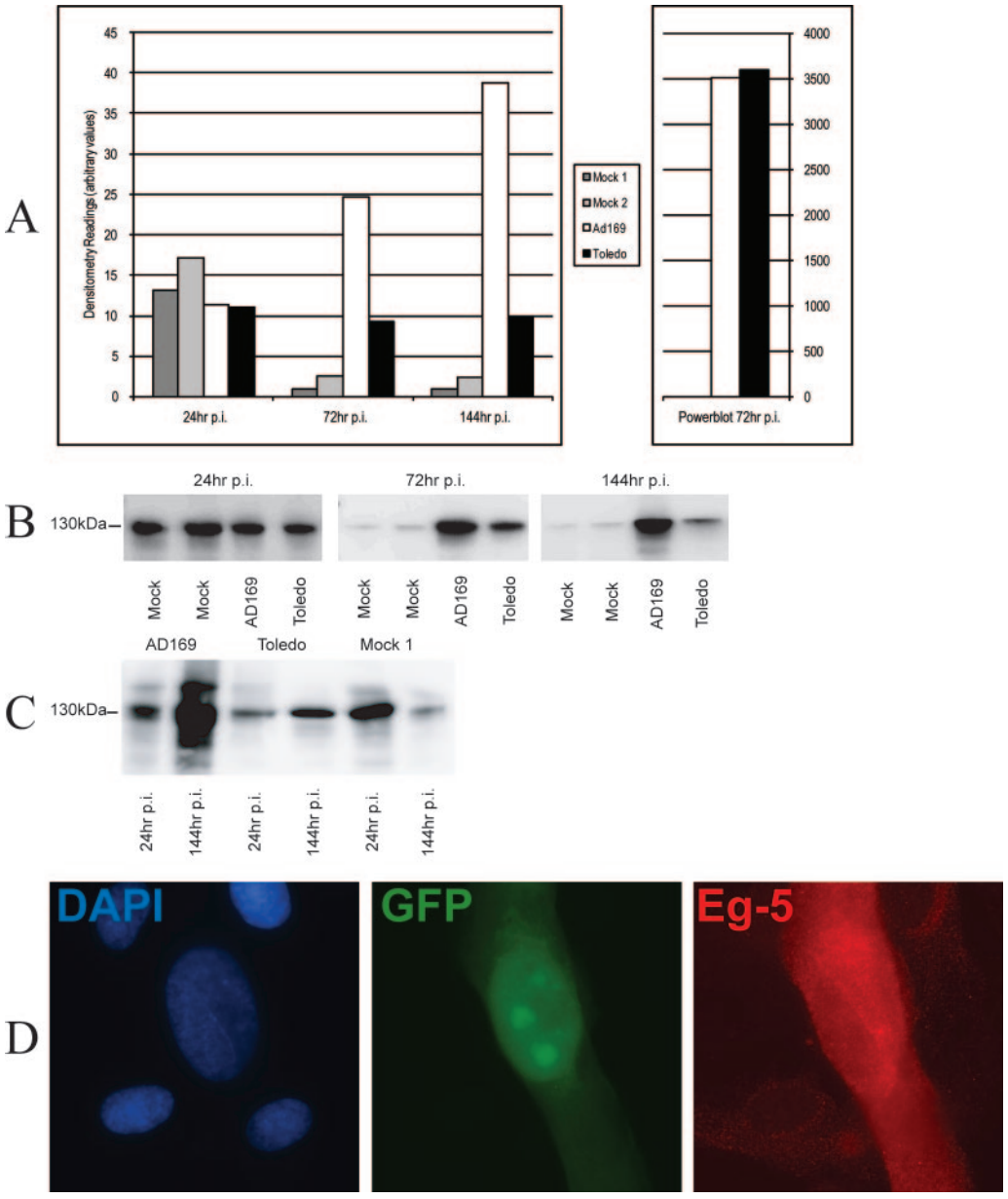


FIG. 2. Analysis of Eg5 expression. (A) Densitometry measurements of Eg5 from conventional Western blot assay data are on the left side of the graph (MOI = 5), and Powerblot data (MOI = 5) are on the right. (B) Conventional Western blotting data from which measurements were taken (MOI = 5). (C) Eg5 levels from different time points on a single blot, allowing direct visual comparison of levels at 24 and 48 hpi. (D) Immunofluorescence assay performed at 48 hpi (MOI = 0.5) with a strain AD169 variant encoding GFP. Staining for Eg-5 is shown in red; DAPI staining of nuclei is in blue.

visualized when cells are plated at a low density on coverslips coated with fibronectin. The structures staining for paxillin in the uninfected cells are characteristic of focal adhesions and were clearly not detectable following HCMV infection. Paxillin became dispersed throughout the cell and exhibited a much more homogeneous cytoplasmic distribution. Identical patterns of disruption of focal adhesions were seen when infections were performed at a low MOI and when strain Toledo-infected cells were stained (data not shown).

**Hic-5 (ARA-55).** Hic-5 is known as an androgen and glucocorticoid receptor coactivator (19, 64) and a negative regulator of muscle differentiation (27). However, Hic-5 also localizes to focal adhesions, is subject to tyrosine phosphorylation, and is similar to paxillin in its primary structure (22, 38, 51). Hic-5 expression was downregulated by 20- to 28-fold following infection with strains AD169 and Toledo in the Powerblot (Fig. 4A). The follow-up Western transfer experiment confirmed that Hic-5 levels were much lower in infected cells than in mock-infected cells. The difference in expression levels was detectable by 24 hpi but much stronger at 72 hpi (7- to 10-fold) and 144 hpi. Interestingly, comparing the different time points indicated that Hic-5 was increasing in mock-infected cells, with

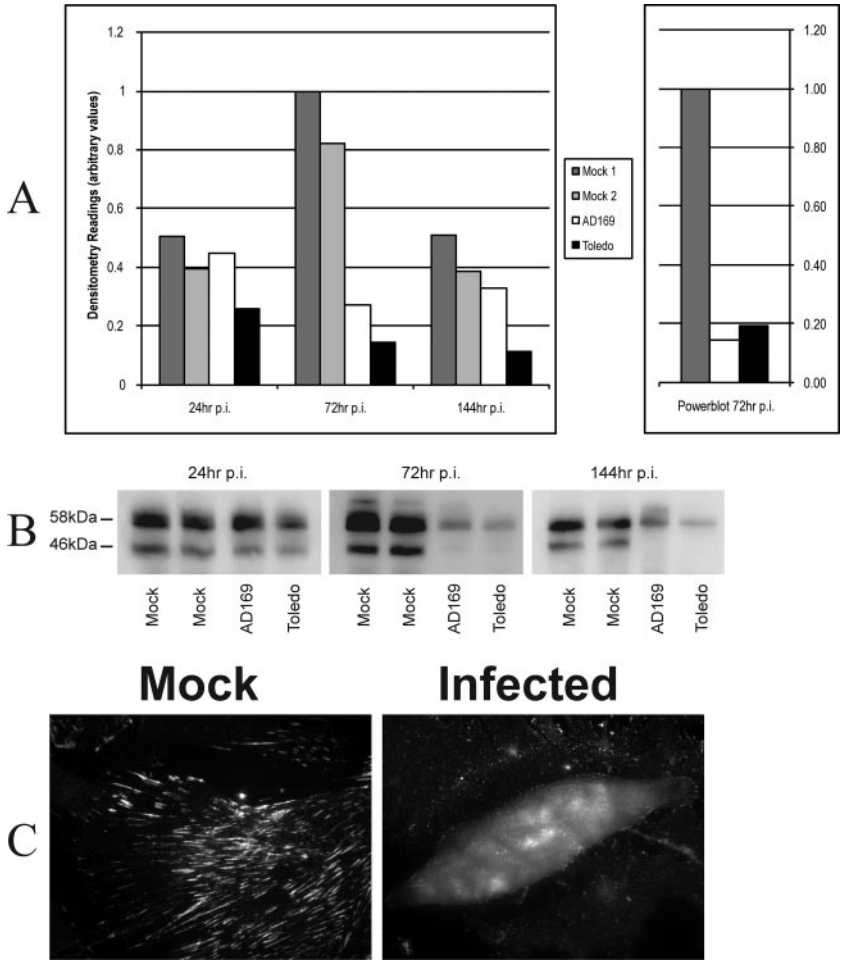


FIG. 3. Analysis of paxillin expression. (A) Densitometry readings from conventional Western blot assays and the Powerblot. Conventional Western blotting data (MOI = 5) are shown on the left for all three of the time points at which measurements were made (24, 72, and 144 hpi); Powerblot data (MOI = 5) were taken at a single time point (72 hpi) and are shown on the right. Only readings for the major 58-kDa band are shown since only this band was present at levels high enough to give accurate readings. (B) Conventional Western blot assays from which the densitometry readings were taken (MOI = 5). (C) Immunofluorescence assay for paxillin performed at 72 hpi (MOI = 5) with a strain AD169 variant or after mock infection.

the reduction in infected cells possibly representing a failure to accumulate rather than active degradation. While the predominant 50-kDa protein and the minor 60-kDa species were both lower during infection, a minor 68-kDa species was not suppressed by HCMV infection. The Hic-5 protein associated with structures typical of focal adhesion in uninfected cells, whereas in infected cells the Hic-5 signal was weaker and was again associated with a general cytoplasmic distribution (Fig. 4C). The Hic-5 staining pattern was also consistent with a disruption of focal adhesions during infection. Experiments performed at both a high MOI and with strain Toledo-infected cells infected at both high and low MOIs showed identical disruptions of focal adhesions in infected cells (data not shown).

**Other focal-adhesion proteins.** Since HCMV infection induced both the dispersal and downregulation of the key focal-adhesion proteins paxillin and Hic-5, we hypothesized that additional proteins associated with focal adhesions may also be displaced. α-Actinin is involved in the binding of the cytoplasmic domain of integrins with actin filaments. Powerblot revealed that α-actinin expression was suppressed in strain Toledo-infected cells (level 9 confidence) and that β1 integrin (CD29) was downregulated in both strain AD169-infected and strain Toledo-infected cells (level 10 confidence). We also investigated the intracellular localization of the major signal transducer associated within the focal adhesions, focal-adhesion kinase (FAK), and α5 integrin (CD49e) in uninfected and strain AD169-infected cells (Fig. 5). A clear difference can be seen between the infected and uninfected cells, with proteins on the cytoplasmic face of the focal adhesions (α-actinin), proteins involved with signal transduction from the focal adhesions (FAK), and the integrins which anchor the focal adhesions to the extracellular matrix (α5/CD49e and β1/CD29 integrins) clearly being displaced upon infection.

**Comparison with microarray data.** The Powerblot generated a data set comparable to that of a microarray, although clearly pertaining to proteins rather than mRNA. A comparison of Powerblot and microarray data has the potential to

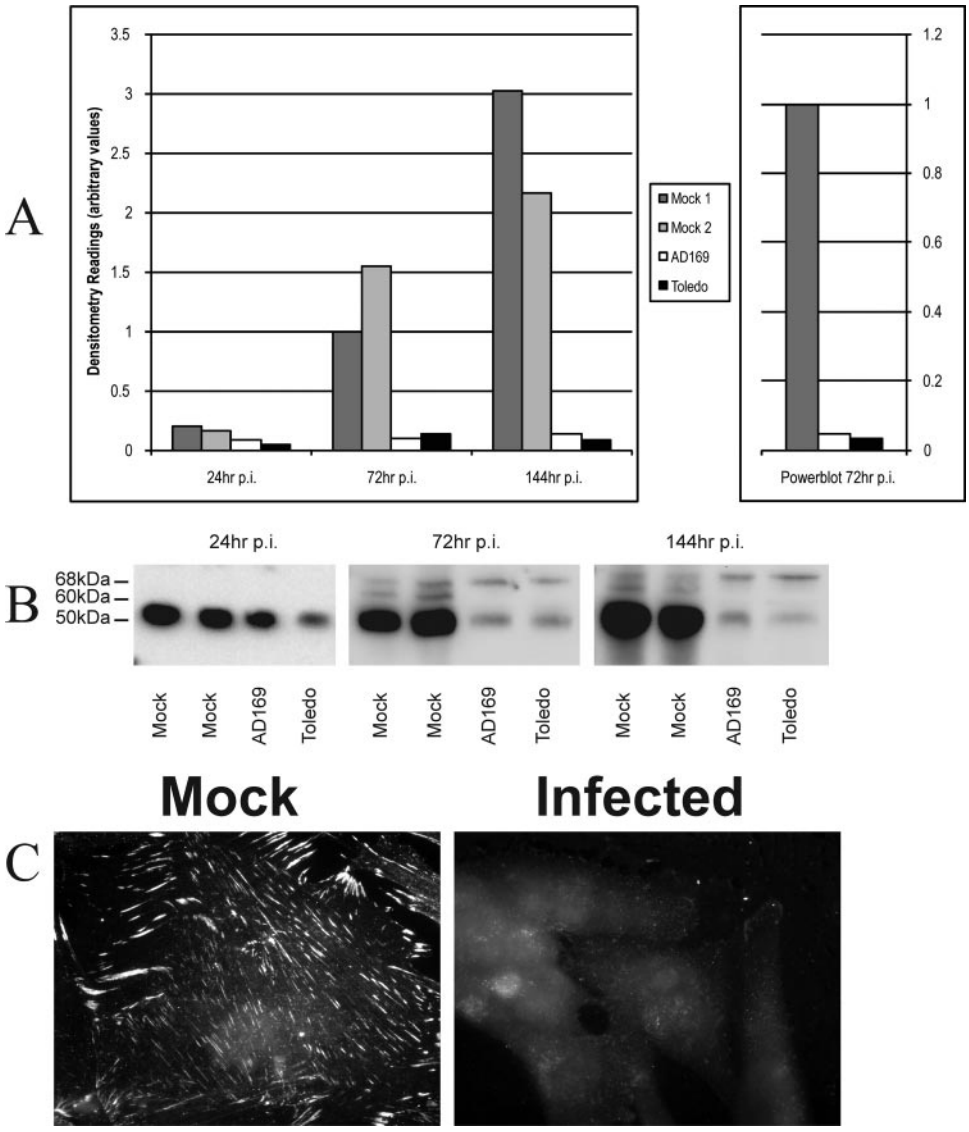


FIG. 4. Analysis of Hic-5 expression. (A) Densitometry readings for Hic-5 levels in conventional Western blot assays (MOI = 5) and the Powerblot (MOI = 5), with conventional Western blotting data on the left and those from the Powerblot on the right. Only levels of the major 58-kDa band are shown since the other bands were too weak to give meaningful measurements. (B) Conventional Western blot assays from which densitometry measurements were taken (MOI = 5). (C) Immunofluorescence assay for Hic-5 performed with HFFF infected 72 h previously with strain AD169-GFP (MOI = 5) or mock infected.

provide insight into the underlying control system regulating cellular gene expression during productive HCMV infection. Published microarray data on strain AD169-infected fibroblasts at 48 hpi (7) and 72 hpi (26) are available. Furthermore, an Affymetrix microarray analysis was performed in our laboratory with RNA harvested at 72 hpi with strain AD169, thereby using conditions identical to those used in the Powerblot (unpublished data). A direct comparison was made between confidence level 10 changes on Powerblot and the three microarray studies. The exact *n*-fold change values were not available for the Hertel and Mocarski data set. Some discrepancies were observed in the microarray data that clearly could be attributable to procedural differences (e.g., fibroblast type, time point, strain AD169 variant, microarray technology). For most of the confidence level 10 protein changes (Table 4), the associated transcripts were found to be static upon HCMV infection: 20/35 (57%) for Hertel and Mocarski, 34/51 (67%) for Browne et al., and 40/49 (82%) for this report. Where a change in steady-state RNA abundance was observed, the direction of the change matched the Powerblot in 11/15 (73%) cases for Hertel and Mocarski, 11/15 (73%) for Browne et al., and 5/9 (56%) for this report. Direct measurements of steady-state RNA and protein levels are therefore not completely compatible, implying a significant element of posttranscriptional or posttranslational control of protein expression during HCMV infection. The Hic-5 transcript decreased in abundance in all three microarrays and by Powerblot, consistent with a protein whose suppression did correlate well with RNA abundance. In the microarray data sets, Eg-5 (three of three) and RIG-G (two of two) were scored as no change whereas

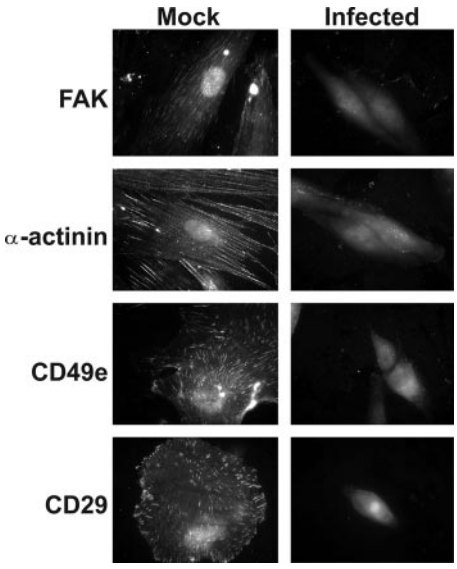


FIG. 5. Immunofluorescence assays performed 72 hpi with strain AD169-GFP (MOI = 5) or after mock infection for focal-adhesion components FAK, α-actinin, CD49e (integrin α5), and CD29 (integrin β1).

protein expression was clearly increased, strongly suggesting that the expression of these two proteins may be regulated at the posttranscriptional level. There are also examples of proteins which showed changes by microarray but not in the Powerblot; for example, Pai-1 and tapasin gave good-quality bands in the Powerblot and were unchanged upon HCMV infection yet were significantly decreased in all three microarray data sets.

## DISCUSSION

Powerblot technology has been used to analyze the effect of HCMV infection on the cellular proteome with more than 1,000 antibodies specific for known proteins. By using Western blot technology, the system ensures that the reaction is against a protein of the appropriate size and can generate data on different isoforms of a single protein. In essence, the Powerblot service is a proteomic screen analogous to a microarray in that it tracks the expression of specific genes. By comparing protein rather than mRNA levels, the readout has potentially greater practical value to virologists. While the Powerblot samples an impressive range of proteins, the technology is constrained to a set collection of antibodies. In contrast, oligonucleotide microarrays have been expanded to permit sampling of steady-state RNA levels for all human genes.

A conservative approach was taken in analyzing the Powerblot data. Since the act of virus infection increases the total amount of protein in the cells, attention was focused on proteins exhibiting a greater-than-twofold difference in abundance. By this criterion, most of the cellular proteome tested remains relatively static during virus infection. Of the 694 proteins that gave a positive signal, only 68 to 71 exhibited a level 10 confidence change in abundance in any one comparison, with slightly more (57 to 63%) increasing than decreasing. Although HCMV is associated with a general activation of cellular gene expression, microarray data report that a minority (21%) of the cellular mRNAs sampled were modulated by HCMV infection at 72 hpi and that the relative abundance of more cellular RNAs was downregulated rather than upregulated during HCMV infection (26). There are many reasons why the modulation of cellular levels of mRNAs need not necessarily translate into measurable changes in the absolute amounts of their protein products. The relative stability of any particular protein is important in this analysis. The synthesis of a protein may be either suppressed or enhanced but not result in an appreciable change in steady-state levels during the course of even a slow virus infection.

The direct comparison between strain AD169-infected and strain Toledo-infected cells identified only 13 proteins changed with the highest confidence (level 10) when cells infected with the two viruses were compared with each other (see Fig. SD in the supplemental material). The magnitudes of Eg-5 and RIG-G activation observed in the more detailed follow-up investigation were both greater with the laboratory-adapted virus. However, despite the reported differences in pathogenesis and genetic makeup of strains AD169 and Toledo, the differential effect on the host proteome was relatively modest. We intend to investigate this aspect further by using both Powerblot and specific antibodies to identify consistent changes attributable to specific gene functions that could be linked with virulence. In this context, the UL/*b′*-encoded NK evasion function UL141 has been shown to retain the activating ligand CD155 in the endoplasmic reticulum as an immature low-molecular-weight precursor. If an antibody specific for CD155 had been included in the array, the retention of CD155 by gpUL141 should have been apparent in the Powerblot analysis. Overall, the Powerblot has proved more instructive than the gene array with respect to strain differences; in the follow-up of a DNA microarray analysis in which 58 cellular genes were analyzed by Northern blotting, all exhibited similar regulation by both HCMV strains AD169 and Toledo (66).

The reliability of the Powerblot data was tested in a follow-up study that used antibodies specific for proteins identified as being modulated by HCMV infection. Visual inspection of the original Powerblot data (available on request) supported the BD computer-aided analyses (see Fig. SB to SD in the supplemental material) of these proteins over the triplicate samples. However, three of the nine proteins initially analyzed exhibited no obvious change in abundance in a conventional Western blot analysis. Although cell extracts were prepared by the same method, some variation in the biological sample is inevitable. The Powerblot requires large protein samples (>4 mg) and is relatively expensive; thus, the system is less amenable to the running of multiple independent biological samples than is microarray technology. The false result obtained with the ZAG antibody also illustrated that the probing of single samples with multiple antibodies to differentially migrating proteins can lead to misinterpretation and reinforces the need to validate the results for specific proteins independently. Nevertheless, for six of the nine proteins we analyzed we were able to validate the Powerblot data. Thus, the Powerblot has generated a large data set for a wide range of cellular proteins that we show here can be usefully tested.

The efficient downregulation of connexin 43 can be expected to have a major impact on intercellular communications in-

TABLE 4. Transcript level changes upon HCMV (AD169) infection taken from microarray data for proteins showing level 10 changes in Powerblot[a]

| Protein | Change in Powerblot | Browne et al | Unpublished Data | Hertel & Mocarski |
|---|---|---|---|---|
| APM | 6.3 | | | D |
| ApoM | -5.0 | MI | NC | |
| Arginase I | -/0 | NC | NC | |
| b-Spectrin II-249KD | -42.7 | NC | D | |
| b-Spectrin II-266KD | -5.7 | NC | D | |
| B56a-55KD | -/0 | NC | | D |
| BUBR1-140KD | 9.1 | NC | NC | |
| Caspase-2/ICH-1L | +/0 | NC | | NC |
| Caspase-3/CPP32 | 3.1 | NC | D | NC |
| CDC5L-96KD? | 2.7 | I | NC | NC |
| CDCrel-1 | -4.3 | | | |
| Cdk7 | 2.8 | | | NC |
| CIP4 | 4.6 | NC | D | |
| Collybistin-132KD? | -9.1 | D | | |
| Connexin-43 | -17.7 | D | NC | D |
| CoRest | 6.0 | | | NC |
| Cyclin B-55KD? | +/0 | I | D | I |
| DBP2 | 4.9 | I | NC | |
| DLP1 | 7.4 | | | |
| Eg5 | +/0 | NC | NC | NC |
| FKBP51 | 4.3 | | | NC |
| FKBP65 | -5.2 | | | D |
| FXR2 | 7.3 | NC | NC | NC |
| Gat | -/0 | | | |
| GIT2-short-58KD | 3.8 | NC | NC | NC |
| GRB2 | 5.8 | MI | NC | NC |
| hCNK1-87KD? | 4.7 | NC | NC | |
| Hic-5-58KD | -31.5 | D | D | D |
| HIP1-136KD? | 3.8 | | | NC |
| Hip1R | +/0 | NC | NC | |
| hPrp16 | 3.1 | MI | D | |
| hPrp17 | 158.7 | MD | NC | |
| ILK | -4.1 | NC | NC | |
| Integrin b1 | -9.0 | NC | NC | D |
| IRAK-99KD | 5.1 | NC | D | NC |
| JBP1/Skb1Hs | -7.2 | | | |
| Karyopherin a/Rch-1 | 7.8 | I | NC | I |
| LAP2 | -3.8 | NC | NC | |
| LSH | 2.9 | | | |
| MCM | -16.3 | NC | NC | I |
| MEK1 | 3.4 | NC | NC | NC |
| N-Copine-67KD? | -14.2 | NC | NC | |
| NHE-1 | +/0 | NC | NC | D |
| nNOS/NOS Type I | +/0 | NC | NC | |
| Nucleoporin p62 | 2.4 | NC | NC | D |
| Nurr-72KD | 5.2 | | | |
| p190 | -13.2 | MI | NC | NC |
| p190 | -4.8 | MI | NC | |
| p19Skp1-23KD? | 2.9 | NC | NC | |
| p43/EMAP II precursor-37KD | 8.4 | | | NC |
| Paxillin-58KD? | -7.3 | NC | NC | D |
| PBK | 13.1 | | NC | |
| PCMT-I/II-33KD? | -5.0 | I | NC | NC |
| PCNA | 5.5 | NC | NC | NC |
| PKAC | -/0 | NC | NC | |
| Rap2 | -7.6 | MD | NC | |
| Rb2-153KD? | -10.4 | NC | NC | NC |
| RIG-G | +/0 | NC | NC | |
| Sam68-67KD | -11.1 | | | D |
| SHC-52KD | -/0 | NC | NC | D |
| Smad2/3 | -/0 | NC | NC | NC |
| Stat3 (pS727), Phospho-Specific-98KD | 6.7 | NC | NC | NC |
| Stat6 | -4.0 | NC | NC | |
| Syntaxin 6 | 5.2 | NC | I | |
| Topo IIa | +/0 | D | NC | I |
| TSC1/Hamartin | 3.2 | MI | NC | |
| ZAP70 Kinase | +/0 | | | |
| Zn-a2-glycoprotein-38KD | -/0 | | | |

[a] NC, no change (medium grey shading); D, decrease (black shading); MD, moderate decrease (black shading); I, increase (light grey shading); MI, moderate increase (light grey shading); +/0, protein increased from undetectable; −/0, protein downmodulated to become undetectable.

volving HCMV-infected cells. Connexin 43 is the predominant connexin expressed in fibroblasts, and it will be interesting to investigate the effect of HCMV infection on additional connexins in cells other than fibroblasts. It will also be important to investigate whether active infection is capable of disrupting established gap junctions. The disassembly of connexin pores could either be a cellular defense to limit virus dissemination or be required by HCMV to prevent the induction of an antiviral state in neighboring cells. The human papillomavirus 16 E5 protein has also been shown to downregulate connexin 43 (41, 52), and thus in this case the disassembly of gap junctions appears to be a viral virulence function rather than a host defense.

HCMV was revealed to have a major effect on proteins associated with the formation of focal adhesions; α-actinin, paxillin, and Hic-5 were all downregulated and, along with FAK, physically dispersed from structures associated with focal adhesions. Depolymerization of actin filaments has long been associated with virion entry and the early phase of infection (30, 37, 59); thus, the breakdown of α-actinin filaments is consistent. The disruption of stress fibers may be anticipated to have an impact on the integrity of adhesion junctions, and the events may be causally linked. Many focal-adhesion proteins have been implicated in the regulation of actin filament reorganization (8, 29, 33, 55), potentially linking the effect with the CPE induced upon CMV infection. In this context, FAK, filamin, and p-190-B were all identified by Powerblot as being suppressed by HCMV infection. Eg5 was selected for follow-up because its expression was enhanced. Although Eg5 expression is reduced when a cell is not actively dividing, it also increases when changes in cellular architecture are occurring (18). This is especially interesting given that Eg5 levels are affected differently in strains AD169 and Toledo, as the CPEs induced by these viruses are known to be distinct (32).

While HCMV suppresses the transcription and expression of components of the extracellular matrix in productive infection, preexisting components appear to persist (28, 47). The Powerblot detects high levels of fibronectin in infected cells, consistent with the extracellular matrix surviving infection. Integrins play a key role in anchoring focal adhesions, directly linking the cytoskeleton with the extracellular matrix. Generally, integrin subunits (α5/CD51, α2/CD49b, α3/CD49c, α5, LFA-1, β4, ICAM-1) generated weak signals in the Powerblot that were not obviously modulated in response to infection. Integrin subunits β1 and β4 were the exception, being identified as being reduced with level 10 and level 9 confidence, respectively, in infected cells. The indication that HCMV downregulates a subset of integrin subunits is consistent with the previously published observation that the virus selectively downregulates α1/β1 integrin (60). Direct examination of the expression of both α5 and β1 integrins by immunofluorescence clearly demonstrated that both were displaced from characteristic focal adhesions during infection.

There was limited concordance between steady-state RNA levels detected by microarray analysis and protein expression detected by Powerblot and follow-up studies. A degree of experimental variation can be expected when comparing RNA microarray or Powerblot studies performed at different times and in different laboratories. Nevertheless, generally, changes in protein expression did not correlate well with RNA abundance, suggesting that the primary mechanism for controlling the abundance of cellular proteins during HCMV infection may not be at the transcriptional level. It was most interesting to see the virus targeting the expression of focal-adhesion proteins as a group, thus presumably disabling all of the associated key cellular functions in cell migration and adhesion associated with these structures. We speculate that once these structures have been disrupted, their component proteins may become vulnerable to proteolysis. Thus, a group of proteins may potentially be controlled en bloc on the post-translational level. Powerblot has defined a substantial set of host cell genes whose expression is modulated during HCMV infection that were not identified by microarray technology. Clearly, the mechanisms responsible for virus control cellular need to be further elaborated. Through the systematic application of HCMV deletion mutants, it may prove possible to identify the HCMV genes responsible for controlling their expression.

## ACKNOWLEDGMENTS

Technical support was kindly provided by S. Llewellyn-Lacey (MRC Co-operative Tissue Culture Facility). Statistical analysis and advice were provided by P. Giles (Department of Pathology, Cardiff University). We are most grateful to Howard Evans and Heather Streeter for helpful discussions and to Richard Randall for cell lines.

This work was funded by a Division of Hospital Specialities Ph.D. studentship and the Wellcome Trust.

## REFERENCES

1. **Adair, R., G. W. Liebisch, Y. Su, and A. M. Colberg-Poley.** 2004. Alteration of cellular RNA splicing and polyadenylation machineries during productive human cytomegalovirus infection. J. Gen. Virol. **85:**3541–3553.
2. **Benedict, C. A., K. D. Butrovich, N. S. Lurain, J. Corbeil, I. Rooney, P. Schneider, J. Tschopp, and C. F. Ware.** 1999. Cutting edge: a novel viral TNF receptor superfamily member in virulent strains of human cytomegalovirus. J. Immunol. **162:**6967–6970.
3. **Biswas, N., V. Sanchez, and D. H. Spector.** 2003. Human cytomegalovirus infection leads to accumulation of geminin and inhibition of the licensing of cellular DNA replication. J. Virol. **77:**2369–2376.
4. **Blangy, A., H. A. Lane, P. d'Herin, M. Harper, M. Kress, and E. A. Nigg.** 1995. Phosphorylation by p34cdc2 regulates spindle association of human Eg5, a kinesin-related motor essential for bipolar spindle formation in vivo. Cell **83:**1159–1169.
5. **Bresnahan, W. A., I. Boldogh, E. A. Thompson, and T. Albrecht.** 1996. Human cytomegalovirus inhibits cellular DNA synthesis and arrests productively infected cells in late $G_1$. Virology **224:**150–160.
6. **Browne, E. P., and T. Shenk.** 2003. Human cytomegalovirus UL83-coded pp65 virion protein inhibits antiviral gene expression in infected cells. Proc. Natl. Acad. Sci. USA **100:**11439–11444.
7. **Browne, E. P., B. Wing, D. Coleman, and T. Shenk.** 2001. Altered cellular mRNA levels in human cytomegalovirus-infected fibroblasts: viral block to the accumulation of antiviral mRNAs. J. Virol. **75:**12319–12330.
8. **Burridge, K., C. E. Turner, and L. H. Romer.** 1992. Tyrosine phosphorylation of paxillin and pp125FAK accompanies cell adhesion to extracellular matrix: a role in cytoskeletal assembly. J. Cell Biol. **119:**893–903.
9. **Cao, J., and A. P. Geballe.** 1996. Inhibition of nascent-peptide release at translation termination. Mol. Cell. Biol. **16:**7109–7114.
10. **Cerboni, C., M. Mousavi-Jazi, A. Linde, K. Soderstrom, M. Brytting, B. Wahren, K. Karre, and E. Carbone.** 2000. Human cytomegalovirus strain-dependent changes in NK cell recognition of infected fibroblasts. J. Immunol. **164:**4775–4782.
11. **Cha, T. A., E. Tom, G. W. Kemble, G. M. Duke, E. S. Mocarski, and R. R. Spaete.** 1996. Human cytomegalovirus clinical isolates carry at least 19 genes not found in laboratory strains. J. Virol. **70:**78–83.
12. **Chalupny, N. J., A. Rein-Weston, S. Dosch, and D. Cosman.** 2006. Down-regulation of the NKG2D ligand MICA by the human cytomegalovirus glycoprotein UL142. Biochem. Biophys. Res. Commun. **346:**175–181.
13. **Compton, T., E. A. Kurt-Jones, K. W. Boehme, J. Belko, E. Latz, D. T. Golenbock, and R. W. Finberg.** 2003. Human cytomegalovirus activates inflammatory cytokine responses via CD14 and Toll-like receptor 2. J. Virol. **77:**4588–4596.
14. **DeMarchi, J. M.** 1983. Post-transcriptional control of human cytomegalovirus gene expression. Virology **124:**390–402.

15. **Dolan, A., C. Cunningham, R. D. Hector, A. F. Hassan-Walker, L. Lee, C. Addison, D. J. Dargan, D. J. McGeoch, D. Gatherer, V. C. Emery, P. D. Griffiths, C. Sinzger, B. P. McSharry, G. W. Wilkinson, and A. J. Davison.** 2004. Genetic content of wild-type human cytomegalovirus. J. Gen. Virol. **85:**1301–1312.
16. **Dunn, W., C. Chou, H. Li, R. Hai, D. Patterson, V. Stolc, H. Zhu, and F. Liu.** 2003. Functional profiling of a human cytomegalovirus genome. Proc. Natl. Acad. Sci. USA **100:**14223–14228.
17. **Dunn, W., P. Trang, Q. Zhong, E. Yang, C. van Belle, and F. Liu.** 2005. Human cytomegalovirus expresses novel microRNAs during productive viral infection. Cell. Microbiol. **7:**1684–1695.
18. **Ferhat, L., C. Cook, M. Chauviere, M. Harper, M. Kress, G. E. Lyons, and P. W. Baas.** 1998. Expression of the mitotic motor protein Eg5 in postmitotic neurons: implications for neuronal development. J. Neurosci. **18:**7822–7835.
19. **Fujimoto, N., S. Yeh, H. Y. Kang, S. Inui, H. C. Chang, A. Mizokami, and C. Chang.** 1999. Cloning and characterization of androgen receptor coactivator, ARA55, in human prostate. J. Biol. Chem. **274:**8316–8321.
20. **Gealy, C., M. Denson, C. Humphreys, B. McSharry, G. Wilkinson, and R. Caswell.** 2005. Posttranscriptional suppression of interleukin-6 production by human cytomegalovirus. J. Virol. **79:**472–485.
21. **Grey, F., A. Antoniewicz, E. Allen, J. Saugstad, A. McShea, J. C. Carrington, and J. Nelson.** 2005. Identification and characterization of human cytomegalovirus-encoded microRNAs. J. Virol. **79:**12095–12099.
22. **Hagmann, J., M. Grob, A. Welman, G. van Willigen, and M. M. Burger.** 1998. Recruitment of the LIM protein hic-5 to focal contacts of human platelets. J. Cell Sci. **111**(Pt. 15)**:**2181–2188.
23. **Hahn, G., M. G. Revello, M. Patrone, E. Percivalle, G. Campanini, A. Sarasini, M. Wagner, A. Gallina, G. Milanesi, U. Koszinowski, F. Baldanti, and G. Gerna.** 2004. Human cytomegalovirus UL131-128 genes are indispensable for virus growth in endothelial cells and virus transfer to leukocytes. J. Virol. **78:**10023–10033.
24. **Heineman, T. C., M. Schleiss, D. I. Bernstein, R. R. Spaete, L. Yan, G. Duke, M. Prichard, Z. Wang, Q. Yan, M. A. Sharp, N. Klein, A. M. Arvin, and G. Kemble.** 2006. A phase 1 study of 4 live, recombinant human cytomegalovirus Towne/Toledo chimeric vaccines. J. Infect. Dis. **193:**1350–1360.
25. **Hertel, L., S. Chou, and E. S. Mocarski.** 2007. Viral and cell cycle-regulated kinases in cytomegalovirus-induced pseudomitosis and replication. PLoS Pathog. **3:**e6.
26. **Hertel, L., and E. S. Mocarski.** 2004. Global analysis of host cell gene expression late during cytomegalovirus infection reveals extensive dysregulation of cell cycle gene expression and induction of pseudomitosis independent of US28 function. J. Virol. **78:**11988–12011.
27. **Hu, Y., P. J. Cascone, L. Cheng, D. Sun, J. R. Nambu, and L. M. Schwartz.** 1999. Lepidopteran DALP, and its mammalian ortholog HIC-5, function as negative regulators of muscle differentiation. Proc. Natl. Acad. Sci. USA **96:**10218–10223.
28. **Ihara, S., S. Saito, and Y. Watanabe.** 1982. Suppression of fibronectin synthesis by an early function(s) of human cytomegalovirus. J. Gen. Virol. **59:**409–413.
29. **Jia, Y., R. F. Ransom, M. Shibanuma, C. Liu, M. J. Welsh, and W. E. Smoyer.** 2001. Identification and characterization of hic-5/ARA55 as an hsp27 binding protein. J. Biol. Chem. **276:**39911–39918.
30. **Jones, N. L., J. C. Lewis, and B. A. Kilpatrick.** 1986. Cytoskeletal disruption during human cytomegalovirus infection of human lung fibroblasts. Eur. J. Cell Biol. **41:**304–312.
31. **Kawaguchi, Y., K. Kato, M. Tanaka, M. Kanamori, Y. Nishiyama, and Y. Yamanashi.** 2003. Conserved protein kinases encoded by herpesviruses and cellular protein kinase cdc2 target the same phosphorylation site in eukaryotic elongation factor 1δ. J. Virol. **77:**2359–2368.
32. **Kemble, G., G. Duke, R. Winter, and R. Spaete.** 1996. Defined large-scale alterations of the human cytomegalovirus genome constructed by cotransfection of overlapping cosmids. J. Virol. **70:**2044–2048.
33. **Leventhal, P. S., and E. L. Feldman.** 1996. Tyrosine phosphorylation and enhanced expression of paxillin during neuronal differentiation in vitro. J. Biol. Chem. **271:**5957–5960.
34. **Lilley, B. N., and H. L. Ploegh.** 2004. A membrane protein required for dislocation of misfolded proteins from the ER. Nature **429:**834–840.
35. **Lischka, P., Z. Toth, M. Thomas, R. Mueller, and T. Stamminger.** 2006. The UL69 transactivator protein of human cytomegalovirus interacts with DEXD/H-Box RNA helicase UAP56 to promote cytoplasmic accumulation of unspliced RNA. Mol. Cell. Biol. **26:**1631–1643.
36. **Liu, B., and M. F. Stinski.** 1992. Human cytomegalovirus contains a tegument protein that enhances transcription from promoters with upstream ATF and AP-1 *cis*-acting elements. J. Virol. **66:**4434–4444.
37. **Lösse, D., R. Lauer, D. Weder, and K. Radsak.** 1982. Actin distribution and synthesis in human fibroblasts infected by cytomegalovirus. Arch. Virol. **71:**353–359.
38. **Matsuya, M., H. Sasaki, H. Aoto, T. Mitaka, K. Nagura, T. Ohba, M. Ishino, S. Takahashi, R. Suzuki, and T. Sasaki.** 1998. Cell adhesion kinase beta forms a complex with a new member, Hic-5, of proteins localized at focal adhesions. J. Biol. Chem. **273:**1003–1014.
39. **McSharry, B. P., C. J. Jones, J. W. Skinner, D. Kipling, and G. W. Wilkinson.** 2001. Human telomerase reverse transcriptase-immortalized MRC-5 and HCA2 human fibroblasts are fully permissive for human cytomegalovirus. J. Gen. Virol. **82:**855–863.
40. **Mocarski, E. S.** 1996. Cytomegalovirus and their replication, p. 2447–2492. *In* B. N. Fields, D. M. Knipe, and P. M. Howley (ed.), Fields virology, 3rd ed. Lippincott-Raven, Philadelphia, PA.
41. **Oelze, I., J. Kartenbeck, K. Crusius, and A. Alonso.** 1995. Human papillomavirus type 16 E5 protein affects cell-cell communication in an epithelial cell line. J. Virol. **69:**4489–4494.
42. **Penfold, M. E., D. J. Dairaghi, G. M. Duke, N. Saederup, E. S. Mocarski, G. W. Kemble, and T. J. Schall.** 1999. Cytomegalovirus encodes a potent alpha chemokine. Proc. Natl. Acad. Sci. USA **96:**9839–9844.
43. **Pfeffer, S., A. Sewer, M. Lagos-Quintana, R. Sheridan, C. Sander, F. A. Grasser, L. F. van Dyk, C. K. Ho, S. Shuman, M. Chien, J. J. Russo, J. Ju, G. Randall, B. D. Lindenbach, C. M. Rice, V. Simon, D. D. Ho, M. Zavolan, and T. Tuschl.** 2005. Identification of microRNAs of the herpesvirus family. Nat. Methods **2:**269–276.
44. **Phillips, A. J., P. Tomasec, E. C. Wang, G. W. Wilkinson, and L. K. Borysiewicz.** 1998. Human cytomegalovirus infection downregulates expression of the cellular aminopeptidases CD10 and CD13. Virology **250:**350–358.
45. **Plotkin, S. A., and W. A. Orenstein.** 2004. Vaccines. Saunders, Philadelphia, PA.
46. **Sambrook, J., and D. Russell.** 2001. Molecular cloning: a laboratory manual, 3rd ed., p. A8.40–A8.51. Cold Spring Harbor Laboratory Press, Cold Spring Harbor, NY.
47. **Schaarschmidt, P., B. Reinhardt, D. Michel, B. Vaida, K. Mayr, A. Luske, R. Baur, J. Gschwend, K. Kleinschmidt, M. Kountidis, U. Wenderoth, R. Voisard, and T. Mertens.** 1999. Altered expression of extracellular matrix in human-cytomegalovirus-infected cells and a human artery organ culture model to study its biological relevance. Intervirology **42:**357–364.
48. **Slobedman, B., J. L. Stern, A. L. Cunningham, A. Abendroth, D. A. Abate, and E. S. Mocarski.** 2004. Impact of human cytomegalovirus latent infection on myeloid progenitor cell gene expression. J. Virol. **78:**4054–4062.
49. **Stanton, R., D. Westmoreland, J. D. Fox, A. J. Davison, and G. W. Wilkinson.** 2005. Stability of human cytomegalovirus genotypes in persistently infected renal transplant recipients. J. Med. Virol. **75:**42–46.
50. **Stinski, M. F.** 1977. Synthesis of proteins and glycoproteins in cells infected with human cytomegalovirus. J. Virol. **23:**751–767.
51. **Thomas, S. M., M. Hagel, and C. E. Turner.** 1999. Characterization of a focal adhesion protein, Hic-5, that shares extensive homology with paxillin. J. Cell Sci. **112**(Pt. 2)**:**181–190.
52. **Tomakidi, P., H. Cheng, A. Kohl, G. Komposch, and A. Alonso.** 2000. Connexin 43 expression is downregulated in raft cultures of human keratinocytes expressing the human papillomavirus type 16 E5 protein. Cell Tissue Res. **301:**323–327.
53. **Tomasec, P., V. M. Braud, C. Rickards, M. B. Powell, B. P. McSharry, S. Gadola, V. Cerundolo, L. K. Borysiewicz, A. J. McMichael, and G. W. Wilkinson.** 2000. Surface expression of HLA-E, an inhibitor of natural killer cells, enhanced by human cytomegalovirus gpUL40. Science **287:**1031.
54. **Tomasec, P., E. C. Wang, A. J. Davison, B. Vojtesek, M. Armstrong, C. Griffin, B. P. McSharry, R. J. Morris, S. Llewellyn-Lacey, C. Rickards, A. Nomoto, C. Sinzger, and G. W. Wilkinson.** 2005. Downregulation of natural killer cell-activating ligand CD155 by human cytomegalovirus UL141. Nat. Immunol. **6:**181–188.
55. **Turner, C. E.** 1994. Paxillin: a cytoskeletal target for tyrosine kinases. Bioessays **16:**47–52.
56. **Turner, C. E., J. R. Glenney, Jr., and K. Burridge.** 1990. Paxillin: a new vinculin-binding protein present in focal adhesions. J. Cell Biol. **111:**1059–1068.
57. **Wang, D., and T. Shenk.** 2005. Human cytomegalovirus virion protein complex required for epithelial and endothelial cell tropism. Proc. Natl. Acad. Sci. USA **102:**18153–18158.
58. **Wang, E. C., B. McSharry, C. Retiere, P. Tomasec, S. Williams, L. K. Borysiewicz, V. M. Braud, and G. W. Wilkinson.** 2002. UL40-mediated NK evasion during productive infection with human cytomegalovirus. Proc. Natl. Acad. Sci. USA **99:**7570–7575.
59. **Wang, X., D. Y. Huang, S. M. Huong, and E. S. Huang.** 2005. Integrin αvβ3 is a coreceptor for human cytomegalovirus. Nat. Med. **11:**515–521.
60. **Warren, A. P., C. N. Owens, L. K. Borysiewicz, and K. Patel.** 1994. Down-regulation of integrin α1/β1 expression and association with cell rounding in human cytomegalovirus-infected fibroblasts. J. Gen. Virol. **75**(Pt. 12)**:**3319–3325.
61. **Welte, S. A., C. Sinzger, S. Z. Lutz, H. Singh-Jasuja, K. L. Sampaio, U. Eknigk, H. G. Rammensee, and A. Steinle.** 2003. Selective intracellular retention of virally induced NKG2D ligands by the human cytomegalovirus UL16 glycoprotein. Eur. J. Immunol. **33:**194–203.
62. **Wills, M. R., O. Ashiru, M. B. Reeves, G. Okecha, J. Trowsdale, P. Tomasec, G. W. Wilkinson, J. Sinclair, and J. G. Sissons.** 2005. Human cytomegalovirus encodes an MHC class I-like molecule (UL142) that functions to inhibit NK cell lysis. J. Immunol. **175:**7457–7465.
63. **Wright, D. A., and D. H. Spector.** 1989. Posttranscriptional regulation of a

class of human cytomegalovirus phosphoproteins encoded by an early transcription unit. J. Virol. **63:**3117–3127.

64. **Yang, L., J. Guerrero, H. Hong, D. B. DeFranco, and M. R. Stallcup.** 2000. Interaction of the tau2 transcriptional activation domain of glucocorticoid receptor with a novel steroid receptor coactivator, Hic-5, which localizes to both focal adhesions and the nuclear matrix. Mol. Biol. Cell **11:**2007–2018.
65. **Zhu, H., J. P. Cong, G. Mamtora, T. Gingeras, and T. Shenk.** 1998. Cellular gene expression altered by human cytomegalovirus: global monitoring with oligonucleotide arrays. Proc. Natl. Acad. Sci. USA **95:**14470–14475.
66. **Zhu, H., J. P. Cong, and T. Shenk.** 1997. Use of differential display analysis to assess the effect of human cytomegalovirus infection on the accumulation of cellular RNAs: induction of interferon-responsive RNAs. Proc. Natl. Acad. Sci. USA **94:**13985–13990.